

Evaluation of Spectrum Occupancy using Approximate and Multiscale Entropy Metrics

Matthias Wellens, Janne Riihijärvi and Petri Mähönen
Department of Wireless Networks, RWTH Aachen University
Kackertstrasse 9, D-52072 Aachen, Germany
Email: {mwe, jar, pma}@mobnets.rwth-aachen.de

Abstract—In this paper we apply approximate and multiscale entropy metrics to spectrum occupancy data gathered during an extensive measurement campaign. We show that the presented methods can be successfully applied to search for and quantify structures of highly varying complexities and time scales. Although structures can be found they are unfortunately relatively complex and it does not appear to be easy to directly exploit them for dynamic spectrum access. We also discuss the major foreseen application areas for entropy-based analysis. These include increasing the reliability of spectrum sensing as well as validation of spectrum occupancy models. Finally, we highlight some results that should be taken into account in future work on spectrum sensing. In particular we observe that strong interference has significant structure, and cannot be well approximated by noise.

I. INTRODUCTION

Dynamic spectrum access (DSA) [1] has become an intensely discussed and studied approach for taking advantage of underutilized licensed frequency bands. The availability of such a technology would greatly alleviate the shortage of radio spectrum helping, for example, the proliferation of services such as community wireless LANs and mesh networks. Detecting and exploiting deterministic structures in the spectrum has been established as a key problem for DSA by several authors [2]–[4]. Appropriate methods could both increase reliability of spectrum sensing itself as well as help in selection of which channels or frequencies to sense more closely for spectrum opportunities.

In this paper we study the use of approximate and multiscale entropy metrics for detecting structure in the spectrum usage. Their major advantage is the ability to find and quantify arbitrary patterns whereas classical techniques such as, e.g., Fourier and correlation analysis tend to discover only periodicities or are bound to certain type of deterministic behaviour. The introduced entropy metrics can instead be used as general complexity measure without assuming anything on the structure to be found.

We apply these techniques to a large collection of measured spectrum occupancy traces and show that they are indeed very promising tools for detecting presence of signals with highly complicated behaviour. To the best of our knowledge this is the first study to apply these entropy metrics in the context of dynamic spectrum access and show that these can effectively quantify complexity of the spectrum usage in different time-scales, enabling differentiation between short-term structures

and long-term changes resulting from user behaviour. Finally, we discuss also the limitations of the presented methods especially focusing on difficulties in distinguishing between strong interference from a user signal in adjacent frequency bands. This appears to be a key problem to tackle in future work on DSA as neither the studied entropy metrics nor other state-of-the-art feature detection mechanisms can deal with strong adjacent-channel interference in a completely satisfactory manner.

The rest of the paper is structured as follows. In Section II we introduce the measurement setup that was used to obtain the studied spectrum occupancy data. We then give in Section III a short tutorial on the entropy metrics applied on the spectrum data in Section IV. We discuss both directions for future work as well as potential applications of these techniques in Section V before drawing the conclusions in Section VI.

II. MEASUREMENT SETUP

The results presented in this paper are based on experimental data gathered during an extensive spectrum occupancy measurement campaign. Here we mostly selected measurement traces from a rather calm radio environment which is representative for a scenario in which a DSA-capable end user device might successfully operate in. The measurement setup was placed on a third-floor balcony of a regular house in a central residential area in Aachen, Germany.

We also present results typical for a busy radio environment as can be found at exposed or other open locations with high number of users close by. We chose a subset of the data measured at a rooftop location on a central university building. Mobile operators have chosen the same location for their base stations because of its good overview over the surroundings. Thus, the signal received at several cellular frequency bands was very strong as it was emitted on the same roof.

The measurement setup itself consisted of an Agilent E4440A high performance spectrum analyzer and a laptop for configuration and data saving purposes enclosed in a weather-proof and RF-shielded wooden box. We used two discone antennas of different sizes and one random antenna to cover the frequency range between 20 MHz and 6 GHz. All antennas are vertically polarized, are omnidirectional in the horizontal plane and have small amount of directivity in the vertical plane. The detailed settings of the spectrum analyzer

TABLE I
SPECTRUM ANALYZER CONFIGURATION USED THROUGHOUT THE
MEASUREMENTS [7].

Center frequency	Subband 1: 770 MHz Subband 2: 2250 MHz Subband 3: 3750 MHz Subband 4: 5250 MHz
Frequency span	1500 MHz
Resolution bandwidth	200 kHz
Number of measurement points	8192
Sweep time	1 s
Measurement duration	≥ 7 days
Detector type	Average detector
Preamplifier	Up to 3 GHz: 28 dB gain, above 3 GHz: ≥ 24 dB gain

are shown in Table I. The selected resolution bandwidth of 200 kHz is a compromise between frequency resolution and the maximum span which can be measured in one sweep. The latter is especially important when large frequency bands should be measured for long time periods as was the case in our campaign. The results presented here are limited to the first two subbands because most real-life systems work in the frequency range between 20 MHz and 3 GHz.

The time between two samples is approximately 1.8 sec and consists of the sweep time of 1 sec and additional overhead for data transfer between the spectrum analyzer and the laptop, and regular instrument realignments. The setup is not able to capture very short structures in the incoming signals such as, e.g., the TV blanking interval. We were interested more in signal structures in time scales of 10s of seconds and longer in order not to have strict synchronization requirements for an end-user DSA device.

Additionally, secondary users will try to limit the time they spend for sensing since these time intervals cannot be used for data transmission in parallel if only a single radio interface is available on the device. In the case of IEEE 802.22 [5], [6] the channel move time is 2 sec which is the major limitation on the time between two consecutive sensing actions. The sampling frequency of our measurement setup is thus on a similar order of magnitude as it will be in such commercial systems.

Further details on the measurement setup and measurement results from different measurement locations are given in [7]–[9].

III. ENTROPY METRICS

We shall now briefly discuss the various entropy metrics used in the study. We begin with Shannon’s information theoretical entropy, highlighting its salient points as well as how it is usually applied to time series. We then move on to discuss two alternative entropies more targeting the characterization of *complexity* than information content. Finally, we discuss multiscale analysis applied to entropy metrics as a potential means for uncovering structures with different time-scales.

In this context a less complex signal would exhibit certain regularity and possibly repeating patterns in the signal over time. The higher the complexity of a time series the less often each pattern will occur in the series, respectively.

A. Classical Information Theoretical Entropy

Given a discrete random variable X , taking values $\{x_1, \dots, x_n\}$ with probabilities $\{p_1, \dots, p_n\}$ we say that the *information content* of an outcome x_i is $-\log p_i$. The *information entropy* or *Shannon entropy* of X is then defined as the mean information content, yielding

$$H(X) \equiv - \sum_{i=1}^n p_i \log p_i. \quad (1)$$

The choice of the base of the logarithm amounts to choice of units. In this paper we have used the natural units obtained by the use of natural logarithm.

Since information entropy has fundamental importance in communications, compression and other areas, it is very natural to use it to estimate the information content of different time series as well. This is usually done by applying (1) on the empirical probabilities obtained from the time series (or in the case of continuous values being measured, on some normalized histogram). Such an approach is perfectly valid in the case the time series is generated by a Markov process [10]. However, if the data has more complicated structure with successive samples being dependent, more intricate analysis is needed. The modern entropy metrics we shall introduce in the following accomplish this by essentially applying (1) not on the data itself, but rather on *sequences* of samples of different lengths.

B. Approximate Entropy

We shall now introduce the *approximate entropy* statistics as defined by Pincus [11]. Let $u(1), \dots, u(N) \in \mathbb{R}$ be our time series. Given a positive constant $m \in N$, we form the vectors $\mathbf{x}(i) \equiv (u(i), \dots, u(i+m-1))$. Each of these vectors has m consecutive values from our original time series starting from $u(i)$. Between two vectors $\mathbf{x}(i)$ and $\mathbf{x}(j)$ we define the distance $d(\mathbf{x}(i), \mathbf{x}(j))$ as the absolute value of the maximum component-wise difference. We then count “similar” vectors by defining

$$C_i^m(r) \equiv \frac{1}{N - m + 1} \#\{j \mid d(\mathbf{x}(i), \mathbf{x}(j)) \leq r\}. \quad (2)$$

The parameter $r \geq 0$ specifies the tolerance for two sequences to be considered similar. Next, we introduce

$$\Phi^m(r) \equiv \frac{1}{N - m + 1} \sum_{i=1}^{N-m+1} \ln C_i^m(r), \quad (3)$$

and, finally, define the *approximate entropy* by

$$\text{ApEn}(m, r) \equiv \lim_{N \rightarrow \infty} (\Phi^m(r) - \Phi^{m+1}(r)). \quad (4)$$

Notice that $\text{ApEn}(m, r)$ can be interpreted as the mean information content of the conditional probability for two subsequences of $u(i)$ that are similar at $m-1$ points continue to be similar for all of m points. This is the connection to information entropy alluded to in the above.

The definition in terms of the infinite limit gives a parameter for describing the underlying process the time series is sampled from. For practical purposes this can be approximated by the statistics

$$\text{ApEn}(m, r, N) \equiv \Phi^m(r) - \Phi^{m+1}(r). \quad (5)$$

Interpretation of the values of these statistics mirrors that of information entropy. Value of zero indicates complete regularity at the length scale of m observation, whereas higher values indicate higher complexity. Comparison of ApEn with different values of m can be used to study the degree of dependency between successive samples. For example, $\text{ApEn}(1, r, N) = \text{ApEn}(2, r, N)$ indicates that the underlying process is (first-order) Markovian.

C. Sample Entropy

Richman and Moorman [12] have pointed out some statistical shortcomings of approximate entropy in the core of time-series analysis. In particular they observed that the length of the time series in question has an impact on the value of ApEn obtained, and that it has a bias originating from self-matches in the above definitions (each sequence is counted as matching itself once). They also proposed a modified version of ApEn, called the *sample entropy*¹ and denoted $\text{SampEn}(m, r, N)$. The interpretation of all the parameters m , r and N is similar to the ApEn case. Since the definition itself is slightly involved and our space is limited we shall not go through the details here. The interested reader is invited to consult [12]. For the applications presented later on it suffices to note that the interpretation of $\text{SampEn}(m, r, N)$ is exactly the same as that of $\text{ApEn}(m, r, N)$.

D. Multiscale Entropy

Both ApEn and SampEn characterize complexity strictly in time-scales defined by the sampling procedure used to obtain the time series under study. Increasing m allows more and more complicated patterns to be detected, but does not make it practical to discover long-term structures in the data. This limitation can be circumvented by the application of multiscale entropy (MSE) analysis introduced by Costa *et al.* in [13], [14]. Their approach consists of forming a coarse-grained time series

$$y_\tau(j) \equiv \frac{1}{\tau} \sum_{i=(j-1)\tau+1}^{j\tau} u(i), \quad (6)$$

where $1 \leq j \leq N/\tau$ and τ is called the *scale factor*, and then applying an entropy metric of interest on $y_\tau(j)$. As a special case $\tau = 1$ the entropy value for the original time series is obtained, whereas higher values of τ correspond to study of behaviour of averages over time windows of length τ . In the following, when MSE analysis is applied to spectrum data, SampEn is always used as an underlying statistic. However, before moving to applications we shall

¹This term should not be confused with the calculation of information entropy from the empirical distribution, which is also occasionally called sample entropy in the literature.

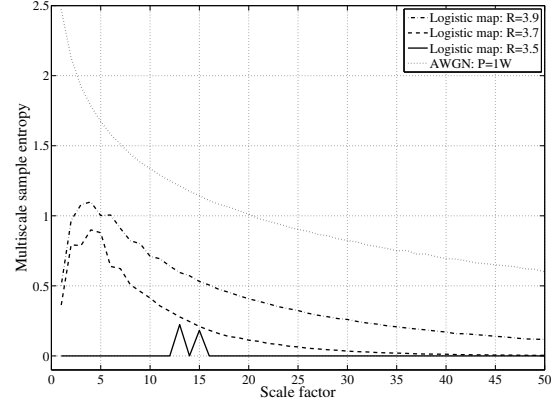


Fig. 1. Multiscale sample entropy computed for the artificial data sets.

briefly illustrate the behaviour of different entropy definitions on some well-understood artificial data sets.

E. Examples for synthetic data

We computed the presented entropy metrics for a collection of artificial data sets. This was done for two reasons. First, since the respective results are available from literature we successfully used these as tests to validate our analysis software. Second, such examples are useful to give insights how the metrics behave for signals of different complexities. We present here selected examples with the following data sets:

- Real valued white gaussian noise with a power of 1 W as a typical model for background noise in communication;
- The iterates of the logistic map $x_{n+1} = Rx_n(1 - x_n)$ with different values for the parameter R . In complexity theory the logistic map is often used as simple model to generate time series of adjustable complexity.

Figure 1 shows the multiscale sample entropy for the introduced artificial time series. Additionally, Table II lists the information theoretical and the approximate entropy. For the logistic map we see that for $R = 3.5$ very low approximate and sample entropies are obtained. This is fully consistent with the known periodic nature of the logistic map with lower values of R . As R is increased more and more complicated behaviour is observed as is witnessed by the increase in both the approximate and sample entropies. Since the distribution of the values of the iterates tends to be close to uniform for large R , information entropy does not distinguish well between $R = 3.7$ and $R = 3.9$. However, the most striking difference is seen when white noise is studied. Due to its unpredictable nature both ApEn and SampEn indicate high level of complexity, whereas information entropy of white noise is actually lower than that of the logistic map for high R . All of these conclusions hold for longer timescales as well as can be seen from Fig. 1.

TABLE II
SHANNON AND APPROXIMATE ENTROPY RESULTS FOR ARTIFICIAL AS WELL AS MEASURED DATA SETS.

Data set	Information theoretical entropy		Approximate entropy				
	32 bins	512 bins	$m = 1$	$m = 2$	$m = 3$	$m = 4$	$m = 5$
Logistic map, $R = 3.9$ (chaotic behaviour)	3.26	5.96	0.60	0.50	0.48	0.48	0.48
Logistic map, $R = 3.7$ (slightly chaotic behaviour)	3.21	5.91	0.48	0.38	0.36	0.36	0.35
Logistic map, $R = 3.5$ (oscillating behaviour)	1.39	1.39	0.00	0.00	0.00	0.00	0.00
White gaussian noise, $P=1$ W	2.80	5.56	2.61	2.48	1.77	0.53	0.06
GSM900 DL, $f=926.3$ MHz, $DC = 5.0\%$, measured trace	1.79	4.52	1.84	1.73	1.60	1.36	0.94
GSM900 DL, $f=958.7$ MHz, $DC = 96.0\%$, measured trace	0.37	1.58	0.59	0.57	0.55	0.52	0.50
GSM900 UL, $f=881.3$ MHz, $DC = 0.2\%$, measured trace	0.13	1.96	1.35	1.29	1.22	1.16	1.07
GSM900 UL, $f=913.7$ MHz, $DC = 9.3\%$, measured trace	0.31	1.68	0.25	0.17	0.15	0.14	0.14
GSM900 DL, $f=926.3$ MHz, $DC = 5.0\%$, binary occupancy trace	0.20	0.20	0.11	0.10	0.10	0.10	0.10
GSM900 DL, $f=958.7$ MHz, $DC = 96.0\%$, binary occupancy trace	0.17	0.17	0.17	0.17	0.17	0.16	0.16
GSM900 UL, $f=881.3$ MHz, $DC = 0.2\%$, binary occupancy trace	0.01	0.01	0.01	0.01	0.01	0.01	0.01
GSM900 UL, $f=913.7$ MHz, $DC = 9.3\%$, binary occupancy trace	0.31	0.31	0.27	0.25	0.25	0.25	0.24

IV. RESULTS

After these examples with synthetic data we continue with presenting some results based on measurement traces taken during the described spectrum occupancy evaluation campaign. We chose traces from frequencies used by popular wireless systems such as cellular networks. We consider time series consisting of the measured received power at a certain frequency channel but also investigate binary occupancy traces.

We define *spectrum occupancy* $\Omega_{t,i}$ at time t and channel index i as follows. We applied energy detection [1], [15] and used a detection threshold of $\gamma = -107$ dBm as given for 200 kHz channels in the requirements document of the IEEE 802.22 standardization committee [6]:

$$\Omega_{t,i} = \begin{cases} 0 & \text{if } P_{rx,t,i} < \gamma \\ 1 & \text{if } P_{rx,t,i} \geq \gamma \end{cases}, \quad (7)$$

where $P_{rx,t,i}$ is the received power. If $\Omega_{t,i} = 1$ the measured channel will be counted as *occupied*, samples with received power below γ indicate a *free* channel, respectively. Furthermore, let us denote N_i as the number of measured samples and DC_i as the duty cycle computed for channel i :

$$DC_i = \frac{\sum_{t=1}^{N_i} \Omega_{t,i}}{N_i}. \quad (8)$$

Usually DC is given in percentage and this is the convention observed in the tables and figures in this paper as well.

During the entropy computations we used $r = 0.15\sigma$ as default parameter value, where σ denotes the standard deviation of the time series under study. This way the entropy values are inherently normalized. Unless noted otherwise we applied $m = 2$ as standard pattern length. These parameter values were tested and found to give good results in our experiments. They are also widely used in the literature [13], [14]. When calculating the information theoretical entropy we also normalized the input time series by the standard deviation.

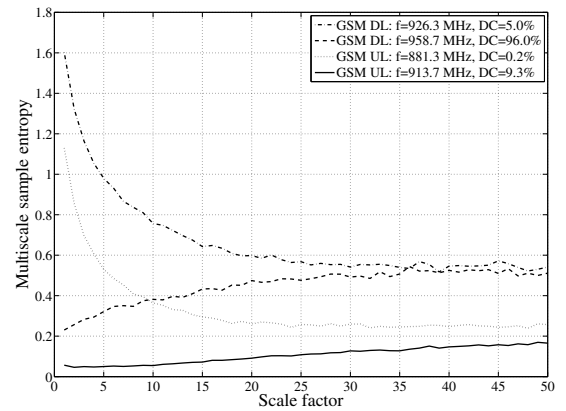


Fig. 2. Multiscale sample entropy computed for 12h of GSM up- and downlink measurement traces.

A. GSM900

As a first example we chose 12 hours (one weekday, from 8:00 am to 8:00 pm) of measurement trace taken in the frequency band regulated for the GSM service. The used resolution bandwidth of 200 kHz corresponds to the signal bandwidth of GSM but the GSM channels and the measurement channels were not aligned. Thus, a single measurement trace may cover up to two neighbouring GSM channels.

Figure 2 shows the multiscale sample entropy for few selected GSM channels. Two types of curves can be differentiated. Traces with lower DC show similar behaviour as white noise although the absolute entropy values are lower for smaller scale factors. Therefore, on shorter time scales the signals exhibit a deterministic structure, which is caused by the underlying on/off processes that describe the usage of the observed channel. The other type of curves corresponds to channels with higher DC . These cases indicate less complexity and especially the drawn through curve for one channel in

the GSM uplink (UL) band goes never above an entropy value of 0.2.

Fully occupied channels ($DC = 100\%$) show less structure and higher entropy values since the measured time series has more noise-like characteristics. The underlying on/off process is always on and the time series thus fluctuates around the average received power but never falls to the background noise level. Instead of the complexity of the on/off process the complexity of the added noise process is evaluated.

B. Comparison of entropies and influence of scale m

Table II lists also the information theoretical and approximate entropy values for selected GSM channels. First thing to observe is the close similarity in the behaviour of information entropy with lower bin count and ApEn when $m = 1$. Even though ApEn and SampEn do not *exactly* reduce to information entropy in low- m limit, they are sufficiently good approximations thereof that it does not appear necessary to separately consider information entropy in future work. Second important observation is the influence of different values of m on the values of ApEn (similar behaviour can be observed for SampEn, but we omit the details for space reasons). For certain data sets (such as the binary occupancy traces) very little change is observed as m is increased. This indicates that there is no further short-term structure in the data than the statistical one already measured by information entropy. However, for several of the raw measurement traces rapidly falling entropy values are observed as m is increased. This in a sense shows that there is significant structure on timescales corresponding to few adjacent measurements. This discussion can of course be extended for the multiscale entropy analysis as well. Different values of m for the aggregated time series would then estimate the amount of structure on time scales of some τ samples. For the measured data increasing m had the effect of reducing multiscale sample entropies throughout, indicating the existence of more complicated structures at longer timescales.

C. GSM1800

We shall now consider the entropies of the frequencies in the upper GSM uplink and downlink bands. Figure 3 shows a time-lag plot of the approximate entropy calculated over a sliding window of three hours for seven days of measured data. We clearly see the expected 24h cycle in the entropy values for both the uplink and the downlink. The high entropy values for the uplink are due to the extremely low duty cycle; the drops in ApEn correspond to traffic being sent in the uplink. If not enough traffic is transmitted at the investigated frequencies the underlying on/off process will be constantly off and the complexity of the background noise process will be evaluated instead. During more active periods ApEn drops showing that if the network carries considerable amount of traffic clear structures can be identified in the signal. For the downlink much more steady traffic stream was observed, which is also indicated by the corresponding entropy values. Overall, for

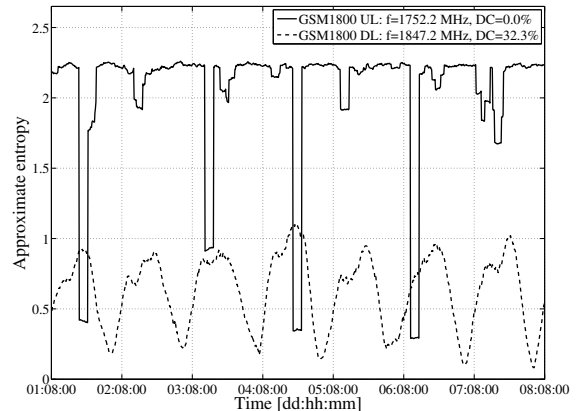


Fig. 3. Approximate entropy computed based on measurements taken during 3h time windows. The investigated time window was moved throughout seven days of available measurement data. The ticks on the x-axis mark 8:00 am on each measurement day.

used GSM channels all the entropy metrics clearly indicate the presence of significant amount of structure.

D. UMTS

As next data set we chose measurement results gathered for the UMTS service. UMTS uses wideband code division multiple access (WCDMA) and thus applies signal spreading to the output signal before transmitting it. Additionally, UMTS base stations will constantly announce their presence using at least the broadcast code and thus emit a continuous signal. Since no feedback is available for these common channels significantly less transmit power adaptations will be conducted by the base stations if no dedicated channels are in use. During our measurements the UMTS uplink channels showed very low duty cycles indicating that broadcast traffic is the dominant factor also in the downlink direction. As consequence of both characteristics a UMTS signal will have noise-like properties to a certain extent. Therefore, we would expect rather high entropy values for UMTS signals.

For the UMTS case we also compared the two measurement locations described in section II. Figure 4 shows the average power spectral density (PSD) measured in the UMTS downlink band at both locations compared to the sensitivity of the deployed measurement setup. The balcony-location is very calm and the different used UMTS channels can clearly be identified. The PSD measured in the other bands is at a similar level as the measurement sensitivity. However, the PSD measured at the rooftop location on the university building is much higher throughout the whole band. The structure of the curve also indicates that some UMTS base stations emit considerable amount of out-of-band interference². This effect

²Although the PSD values measured on the roof of the university building were the highest of all measurement locations we also measured strong out-of-band interference at other more exposed locations [7].

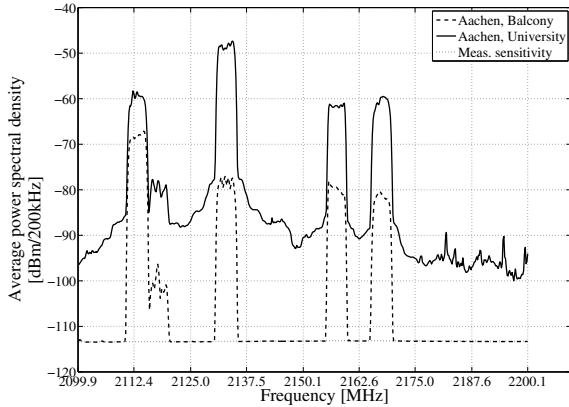


Fig. 4. Comparison of average power spectral density received at two measurement locations throughout the whole measurement.

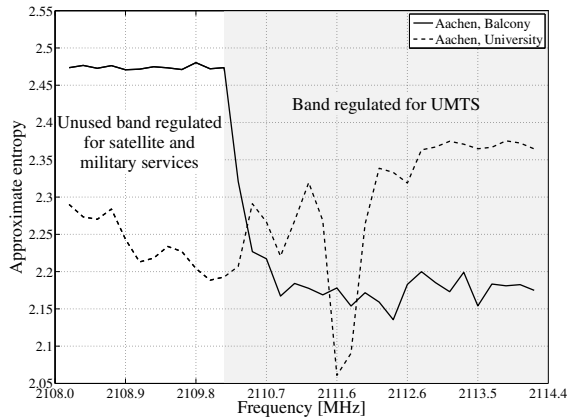


Fig. 5. Comparison of the approximate entropy computed for 12h of measurement traces taken in parts of the UMTS and an adjacent band. Results for measurements taken at two different measurement locations are shown.

could be captured at that location because few cellular base stations were installed on the same roof.

Figure 5 shows the approximate entropy over frequency for a specifically selected frequency band. The first couple of channels do not belong to the regulated UMTS frequency band and were most probably not used at either of the measurement locations. The remaining channels (the shaded area) belong to the frequency band licensed for UMTS services. The total numbers of the approximate entropy are high for all shown channels confirming our expectations because of the underlying signal spreading technology. Nevertheless, the difference between the pure noise and the UMTS signal is clearly visible for the results measured in the calm radio environment at the balcony location. However, in the noisy environment at the university building no clear difference can be seen.

Figure 6 shows the multiscale sample entropy for two example channels taken from the two spectrum bands and the calm radio environment. Both curves have shapes similar to the

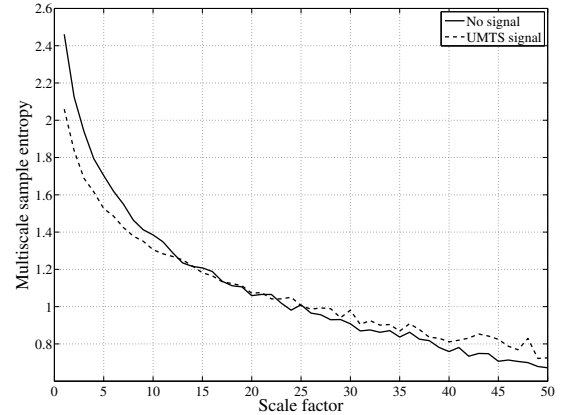


Fig. 6. Multiscale sample entropy computed for 12h of measurement traces. Both curves are examples for channels in the UMTS band and an adjacent band.

curve we showed for white noise in section III-E. Similarly to ApEn also the SampEn (multiscale sample entropy for scale factor = 1) shows the difference between the UMTS signal and the noise. If longer parts of the measurement traces are combined the situation changes and the entropy is slightly lower in the case of the noise signal.

We can conclude that the UMTS signal exhibits little short-term structure that enables differentiation from noise in some cases. Since the total numbers of the entropy metrics are high the UMTS signal is still not a good candidate for simple exploitation of signal structures. Additionally, the same structure is also present in out-of-band transmissions that can be received near a base station or at very exposed locations.

V. DISCUSSION

The entropy metrics studied all appear to be effective in detecting structure in spectrum occupancy data. Varying the values of the m -parameter as well as applying the multiscale entropy analysis also allows to flexibly study structures of varying complexities and timescales. These findings confirm the initial results reported in [2]–[4] that proposed to exploit structures in spectrum for more efficient DSA systems. However, it should be pointed out that actually taking advantage of these structures is highly non-trivial. As was also shown in earlier work [8] simple approaches such as trying to discover periodicities in the spectrum occupancy do not appear to work well. This is consistent with the non-zero entropy values even with high m -values.

It should be noted that all these comments only apply to the time scales studied in the measurements. For shorter timescales (on the order of single frames or timeslots) potentially much more structure would be present, but confirming this expectation and studying its potential applications are beyond the scope of this paper. It should also be noted that taking advantage of structures in shorter timescales would require rather strict synchronization of secondary users to the primary

user, potentially limiting the usefulness of the detection of such structures. Additionally, secondary users have to be highly confident that the observed primary user time pattern does not change during the secondary data transmission period in order to avoid harmful interference. Such confidence levels may only be achievable if prior knowledge on the structure of the primary user traffic is available. If this is the case specifically designed test and tracking procedures will be more efficient than general search for signal structure based on, e.g., entropy metrics.

Even though direct exploitation of the structure in spectrum as indicated by the multiscale entropy analysis appears to be difficult, we foresee two important application areas for these methods. First of all we believe that entropy analysis can be used to select frequency bands for more detailed scanning, whether by means of technology-specific techniques [16] or methods such as cyclostationary feature detection [17]. Refined measurement setups, e.g., using faster sampling rate, may also enable regulatory bodies to apply entropy measures for generic evaluation of spectrum usage. With the exception of noise-like behaviour of UMTS signals, structure in all other bands was very clearly detected in all the cases traffic was present in the band. Even in the case of UMTS slight departure from noise was observable in low-noise environment, but this departure is too slight to rely on in the general case.

It was also interesting to observe that strong interference appeared to exhibit a great deal of structure, and in general behaved more like a signal than strong noise source. This obviously poses another limitation for use of entropy-type methods for signal detection on long timescales, but also highlights the need for further research in general feature detection as interference clearly cannot be considered as noise, as was also recently pointed out by other researchers, see, e.g., [18].

The second major application area we foresee for entropy metrics is validation of spectrum occupancy models. For example, simple first-order Markov models for spectrum occupancy would have $\text{ApEn}(1, r, N) = \text{ApEn}(m, r, N)$ for all $m \geq 1$. Similarly, comparing the entropies of the measured data and a realisation of the model can be used as a rough metric for goodness-of-fit. For a more detailed discussion focussing on Markov models of various orders we refer the reader to [19]. Construction of realistic spectrum occupancy models is a part of our future work, and we expect entropy metrics to serve as powerful tools in the process.

VI. CONCLUSION

We studied the use of entropy metrics in characterizing the complexity of and discovering structures in spectrum data. Rich structures of varying time scales and lengths of observed sequences were found in the data, indicating that the entropy metrics discussed definitely warrant further study in this application area. We also discussed potential applications at some length, clear candidates being assisting in selection of frequency bands for further scanning, as well as validation of

models for spectrum occupancy. We intend to pursue both of these avenues in our future work.

ACKNOWLEDGMENT

The authors would like to thank RWTH Aachen University and the German Research Foundation (Deutsche Forschungsgemeinschaft, DFG) for providing financial support through the UMIC excellence cluster. We would also like to thank European Union for providing partial funding of this work through the ARAGORN project. Additionally, we would like to thank Marten Bandholz and Sonja Bone, and RWTH Aachen University for providing us access to the outdoor measurement locations and Jin Wu and Gero Schmidt-Kärst for practical support during some of the measurements and for constructing the weather-proof box. Finally, we would like to thank Alexandre de Baynast for insightful and exciting discussions in the context of dynamic spectrum access.

REFERENCES

- [1] I. F. Akyildiz, W.-Y. Lee, M. C. Vuran, and S. Mohanty, "Next generation/dynamic spectrum access/cognitive radio wireless networks: a survey," *Elsevier Computer Networks Journal*, vol. 50, no. 13, pp. 2127–2159, September 2006.
- [2] K. Challapali, S. Mangold, and Z. Zhong, "Spectrum agile radio: detecting spectrum opportunities," in *Proc. of International Symposium on Advanced Radio Technologies (ISART)*, Boulder, CO, USA, March 2004.
- [3] S. Mangold, Z. Zhong, K. Challapali, and C.-T. Chou, "Spectrum agile radio: radio resource measurements for opportunistic spectrum usage," in *Proc. of IEEE Global Telecommunications Conference (GLOBECOM)*, vol. 6, Dallas, TX, USA, December 2004, pp. 3467–3471.
- [4] S. Geirhofer, L. Tong, and B. M. Sadler, "Dynamic spectrum access in the time domain: modeling and exploiting white space," *IEEE Communications Magazine*, vol. 45, no. 5, pp. 66–72, May 2007.
- [5] C. Cordeiro, K. Challapali, D. Birru, and S. Shankar, "IEEE 802.22: An Introduction to the First Wireless Standard based on Cognitive Radios," *Journal of Communications*, vol. 1, no. 1, pp. 38–47, April 2006.
- [6] S. Shellhammer and G. Chouinard, "Spectrum sensing requirements summary," IEEE 802.22-05/22-06-0089-05-0000, July 2006.
- [7] M. Wellens, J. Wu, and P. Mähönen, "Evaluation of spectrum occupancy in indoor and outdoor scenario in the context of cognitive radio," in *Proc. of CROWNCOM*, Orlando, FL, USA, August 2007.
- [8] M. Wellens, A. de Baynast, and P. Mähönen, "Exploiting Historical Spectrum Occupancy Information for Adaptive Spectrum Sensing," in *Proc. of IEEE Wireless Communications and Networking Conference (WCNC)*, Las Vegas, NV, USA, April 2008.
- [9] —, "On the Performance of Dynamic Spectrum Access based on Spectrum Occupancy Statistics," *accepted for publication in IET Communications, Special Issue on Cognitive Spectrum Access*, 2008.
- [10] C. E. Shannon, "A Mathematical Theory of Communication," *The Bell System Technical Journal*, vol. 27, no. 4, pp. 379–423, July 1948.
- [11] S. Pincus, "Approximate entropy as a measure of system complexity," *Proceedings of the National Academy of Sciences of the United States of America*, vol. 88, no. 6, pp. 2297–2301, March 1991.
- [12] J. Richman and J. Moorman, "Physiological time-series analysis using approximate entropy and sample entropy," *American Journal of Physiology- Heart and Circulatory Physiology*, vol. 278, no. 6, pp. 2039–2049, 2000.
- [13] M. Costa, A. L. Goldberger, and C.-K. Peng, "Multiscale Entropy Analysis of Complex Physiologic Time Series," *Physical Review Letters*, vol. 89, no. 6, p. 068102, August 2002.
- [14] —, "Multiscale entropy analysis of biological signals," *Physical Review E*, vol. 71, no. 2, p. 021906, February 2005.
- [15] D. Cabric, A. Tkachenko, and R. W. Brodersen, "Experimental Study of Spectrum Sensing based on Energy Detection and Network Cooperation," in *Proc. of Workshop on Technology and Policy for Accessing Spectrum (TAPAS)*, Boston, MA, USA, August 2006.

- [16] C. Cordeiro, M. Ghosh, D. Cavalcanti, and K. Challapali, "Spectrum Sensing for Dynamic Spectrum Access of TV Bands," in *Proc. of CROWNCOM*, Orlando, FL, USA, August 2007.
- [17] W. A. Gardner, "Signal interception: A unifying theoretical framework for feature detection," *IEEE Transactions on Communications*, vol. 36, no. 8, pp. 897–906, August 1988.
- [18] R. Tandra and A. Sahai, "SNR Walls for signal detection," *IEEE Journal on Special Topics in Signal Processing*, vol. 2, no. 1, pp. 4–17, February 2008.
- [19] S. Pincus, "Approximating Markov Chains," *Proceedings of the National Academy of Sciences of the United States of America*, vol. 89, no. 10, pp. 4432–4436, 1992.